CrossMark

Synthesis of multifunction optical filter based on digital signal processing method

Juan Zhang[1] · Yang Wang[2]

Abstract By a digital signal processing method, a multifunction optical filter is synthesized. The filter is formed by a Mach–Zehnder interferometer with two cascaded double-ring resonators and a single-ring resonator on the two arms respectively. It can operate as a symmetrical interleaver, an asymmetrical interleaver with arbitrary duty cycles, a notch filter with a single notch point and a notch filter with two notch points. These four functions can be realized by choosing appropriate structural parameters. The configurable and tunable features make it useful in the future intelligent optical communication networks.

Keywords Optical interleaver · Optical notch filter · Ring resonator · Z-transform

1 Introduction

Multifunction optical filters (Dingel and Izutsu 1998; Dingel 2014) are key components in the next-generation intelligent optical networks, which provide configurable and programmable features (Modarrerssi and Mohan 2000). Optical filters with simple configurations are necessary for a compact, versatile and economical dense wavelength division multiplexed (DWDM) system. Optical ring resonator is the most widely used basic block in various application systems, such as optical interconnect (Xia et al. 2007), optical

✉ Juan Zhang
juanzhang@staff.shu.edu.cn

Yang Wang
ywang@siom.ac.cn

1   Key Laboratory of Specialty Fiber Optics and Optical Access Networks, School of Communication and Information Engineering, Shanghai University, Shanghai 200072, China

2   Shanghai Institute of Optics and Fine Mechanics, Chinese Academy of Sciences, Shanghai 201800, China

communication (Little et al. 2004), optical sensing (Sun and Fan 2011), optical signal processing and so on. Due to their ability to provide wavelength selectivity, and easily cascadable, the optical ring resonators have great potential for allowing the realization of various filter responses, which is the basis of multifunctional filtering.

The synthesis and analysis of ring-resonator type multifunction filters is still a rather challenging task. Numerous phases, delays, and coupling parameters need to be controlled. In recent years, researchers in optics have paid increasing attentions on the digital signal processing (DSP) technology because it brings about new solutions to some important optical signal processing issues (Cheng 2006; Zhang 2016). Some optical filters can be designed based on DSP methods due to the similar feedback characteristics of optical and digital filters (Madsen and Zhao 1999; Yang and Zhang 2008; Cheng and Tang 2013; Madsen 2000; Zhang and Yang 2010; Zhang et al. 2012, 2014; Pinzon et al. 2013). Compared with the complex optical interferometric analysis, DSP-based design methods are more simple and effective because many mature computer-based DSP algorithms and technologies can be directly used.

In this paper, we demonstrate the use of a DSP method to the synthesis of a ring-resonator based multifunctional optical filter. The proposed structure is an unbalanced Mach–Zehnder interferometer (MZI) with coupled ring resonators. The multifunction optical filter can function as symmetrical interleaver, asymmetrical interleaver with arbitrary duty cycles, notch filter with a single notch point, and notch filter with two notch points, depending on the parameters of the structure.

2 Optical structure and digital signal model

Figure 1 shows the schematic structure of the multifunction filter. It is formed by a Mach–Zehnder interferometer (MZI) with two cascaded serially coupled double-ring resonators and a single-ring resonator coupled on the arm 1 and arm 2 respectively. On arm 1, the coupling coefficients of the first double-ring resonators are K_{11}, K_{12} and the corresponding ring lengths are l_{11}, l_{12}, respectively. The coupling coefficients of the second double-ring resonators are K_{21}, K_{22} and the corresponding ring lengths are l_{21}, l_{22}, respectively. On arm 2, the coupling coefficient and ring length of the single-ring resonator are K_L and L_L respectively. ΔL (= $L_1 - L_2$) is the length difference of the two arms of the MZI. K_a and K_b ($K_a = K_b = 0.5$) are the coupling coefficients of the 3 dB couplers in the input and output ports of the MZI respectively.

Fig. 1 Schematic of the proposed multifunction filter
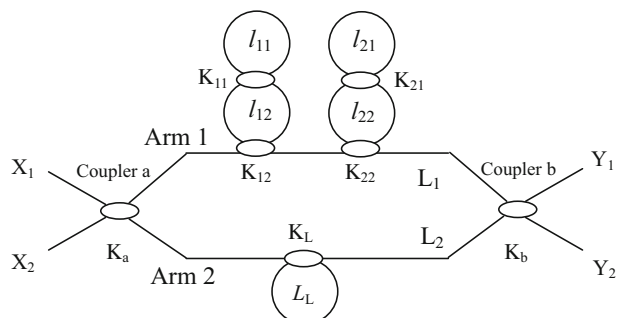
The optical structure shown in Fig. 1 can be transformed into a digital signal model by the Z-transform method, as shown in Fig. 2. The equivalence of the optical and signal parameters can be shown as $c_a = (1 - K_a)^{1/2}$, $s_a = (K_a)^{1/2}$, $c_b = (1 - K_b)^{1/2}$ and $s_b = (K_b)^{1/2}$. $e^{-j\varphi} = e^{-j\beta\Delta L}$ is the phase shift produced by the MZI, where $\beta = 2\pi n_e/\lambda$, n_e is the effective refractive index of medium, and λ is the wavelength in vacuum. $H_{dou}^1(z)$ and $H_{dou}^2(z)$ are the transfer functions of the first and second double-ring resonator in the upper arm respectively. $H_{sin}(z)$ is the transfer functions of the single-ring resonator in the lower arm.

The proposed model of the multifunction filter is different from the available published models of interleavers or notch filters in the following two aspects. First, it uses two serially coupled ring resonators, rather than commonly-used (cascaded) single rings in one arm of the MZI. Second, no phase shifter is needed on each ring. Multifunction filter can be realized only by choosing appropriate values of the path length differences of the MZI, ring length of the resonators, and the coupling coefficients of the couplers. Figure 3 shows the Z-transform schematics of the single-ring and serially coupled double-ring resonator respectively.

The transfer function of the single-ring resonator can be obtained from Fig. 3a as

$$H_d(z) = H_{sin}(z) = \frac{z^{-1} - c_L}{c_L z^{-1} - 1}. \tag{1}$$

here $c_L = (1 - K_L)^{1/2}$. From Fig. 3b, we can get the transfer function of the double-ring resonator by recursion as (Zhang 2016)
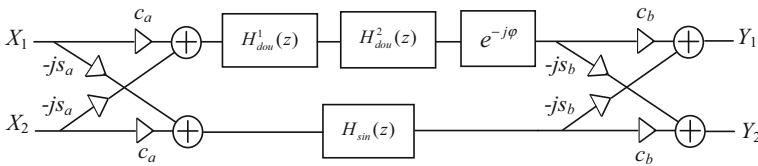

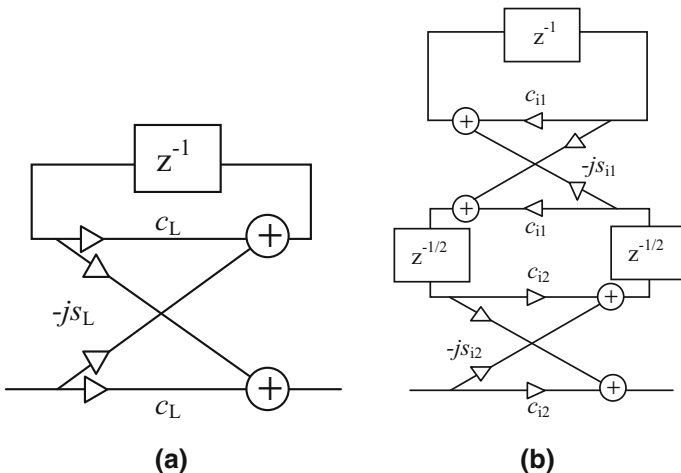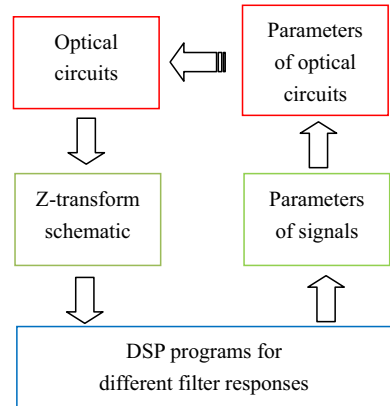**Fig. 2** Digital signal model of the proposed multifunction filter

Fig. 3 Z-transform schematics of **a** single-ring resonator, **b** serially coupled double-ring resonators

Fig. 4 Schematic process of synthesizing the multifunction filter based on a DSP method

$$H_{dou}^i(z) = \frac{z^{-2} - c_{i1}(1 + c_{i2})z^{-1} + c_{i2}}{c_{i2}z^{-2} - c_{i1}(1 + c_{i2})z^{-1} + 1}, \quad (i = 1, 2) \tag{2}$$

here $c_{i1} = (1 - K_{i1})^{1/2}$ and $c_{i2} = (1 - K_{i2})^{1/2}$, thus the transfer function of two cascaded double-ring resonators can be denoted as

$$H_u(z) = H_{dou}^1(z) \times H_{dou}^2(z), \tag{3}$$

where $z^{-1} = e^{-j\omega} = e^{-j(2\pi n e L)/\lambda}$, $L = C/(\Delta f \cdot n_e)$, L is the unit ring length, Δf is the spectral period and C is the speed of light in vacuum.

According to Fig. 2, we can obtain the transfer function of the whole structure as follows:

$$H_1(z) = \frac{Y_1}{X_1} = \frac{1}{2}\left[H_u(z) \cdot z^{-\frac{\Delta L}{L}} - H_d(z)\right], \tag{4}$$

$$H_2(z) = \frac{Y_2}{X_1} = -j\frac{1}{2}\left[H_u(z) \cdot z^{-\frac{\Delta L}{L}} + H_d(z)\right]. \tag{5}$$

Different filter responses to achieve multi-functions can be obtained by changing the transfer functions. Then the corresponding structural parameters can be deduced. The schematic process for synthesizing the multifunction filters is shown in Fig. 4.

3 Multifunction filtering characteristics

3.1 Optical interleavers

The poles of $H_1(z)$ (or $H_2(z)$) must be conjugate pairs on the imaginary axis to form a symmetrical interleaver, otherwise asymmetrical spectra can be obtained (Zhang and Yang 2010). According to this design theory, symmetrical interleaver and asymmetrical interleaver with arbitrary duty cycles can be synthesized.

Firstly, the structure can function as a symmetrical interleaver when $K_{21} = K_{22} = 0$, $\Delta L = L$ and $l_{11} = l_{12} = L_L = 2\Delta L$. Choosing appropriate coupling coefficients of the first double-ring resonator and the single-ring resonator, a flat-top spectral response can be
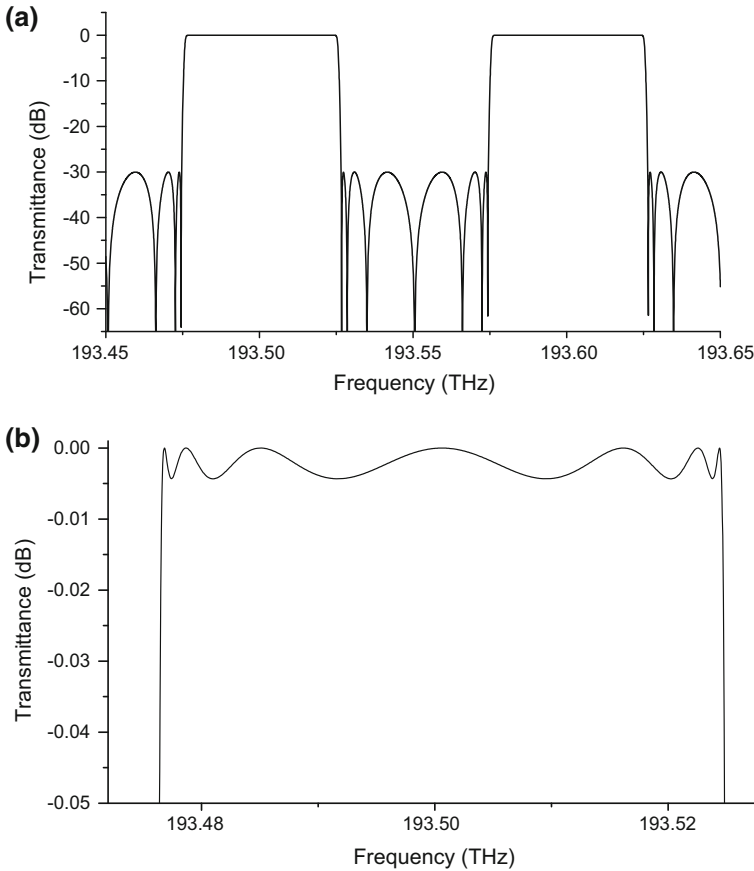
Fig. 5 Transmission spectra of a symmetrical interleaver. **a** transmission spectrum as the function of frequency. **b** zoomed passband

obtained. Figure 5a shows the transmission spectrum as the function of frequency with $K_{11} = 0.08358$, $K_{12} = 0.93041$ and $K_L = 0.51442$. The detailed passband spectrum is shown in Fig. 5b. The ripple of the flat-top equals to 0.00432 dB, i.e. the isolation equals to 30.04 dB. The rectangle degree, defined as the ratio of the channel width at 3 dB to 20 dB, is calculated to be 0.970. As we know, the larger the rectangle degree, the better the filtering performance of the interleaver.

Secondly, the structure can also function as an asymmetrical interleaver with arbitrary duty cycles. It is known that an optical interleaver can be viewed as a lowpass-highpass doubly-complementary filter pair. In DSP theory, an odd order lowpass-highpass doubly-complementary filter pair can always be decomposed into sum or difference of two all-pass filters with adjacent orders (Mitra 2006). Therefore, from Eqs. (4) and (5), we can see that interleavers with arbitrary duty cycles can be synthesized by decomposing transfer functions into sum or difference of the all-pass filters with adjacent orders when ΔL equals to zero. According to this design theory, the structure can function as asymmetrical inter-leaver with arbitrary duty cycle when $K_{21} = K_{22} = 0$, $\Delta L = 0$ and $l_{11} = l_{12} = l_{21} = l_{22} = L_L = L$.

Figure 6 shows the output spectra of the asymmetrical interleavers as the function of frequency with four different duty cycles. The corresponding structural parameters are shown in Table 1 in detail. Table 2 shows the 3 dB, 20 dB bandwidth and the rectangle degree of the asymmetrical interleavers for the two output ports. It can be seen that flat-top profile and high isolation can be obtained for the two output ports at the same time. Moreover, the rectangle degree for the wide output port is always larger than that for the narrow output port with the same duty cycle. The rectangle degree of the symmetrical
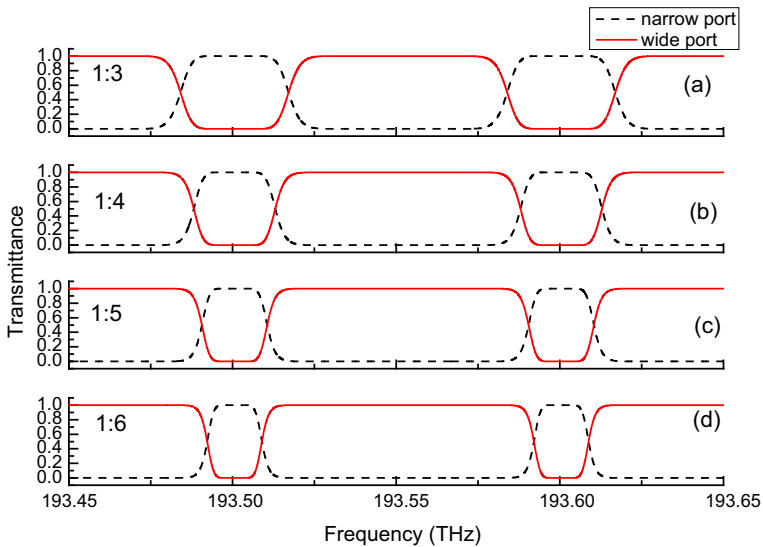

Fig. 6 Output spectra of the two output ports with the duty cycle of **a** 1:3 **b** 1:4 **c** 1:5 **d** 1:6

Table 1 Coupling coefficients of the resonators for the asymmetrical interleavers with different duty cycles

Duty cycle	1:3	1:4	1:5	1:6
Coupling coefficients	$K_{11} = 0.74109$ $K_{12} = 0.76801$ $K_{21} = 0.92533$	$K_{11} = 0.49818$ $K_{12} = 0.69286$ $K_{21} = 0.82768$	$K_{11} = 0.34560$ $K_{12} = 0.62259$ $K_{21} = 0.74059$	$K_{11} = 0.25245$ $K_{12} = 0.56324$ $K_{21} = 0.66897$

Table 2 Bandwidths and rectangle degrees of the asymmetrical interleavers with different duty cycles for the narrow and wide output ports

Duty cycles	Narrow output port			Wide output port		
	3 dB bandwidth (GHz)	20 dB bandwidth (GHz)	Rectangle degree	3 dB bandwidth (GHz)	20 dB bandwidth (GHz)	Rectangle degree
1:3	33.01	48.99	0.674	66.78	79.17	0.844
1:4	24.88	39.18	0.635	74.91	84.66	0.885
1:5	19.97	32.06	0.623	79.89	87.86	0.909
1:6	16.71	27.27	0.613	83.09	89.81	0.925

interleaver is higher than that of the asymmetrical interleaver due to the higher filter order of the former. The symmetrical interleaver is a seven-order filter, whereas the asymmetrical interleaver is a three-order filter. Asymmetrical interleavers with higher rectangle degrees can be obtained by increasing the number of coupled optical rings.

3.2 Optical notch filters

The optical notch filter can be transformed into an allpass filter as $H(z) = 1/2(1 + A(z))$, where $A(z)$ is an allpass filter (Pei and Tseng 1997). Therefore, the structure can function as a notch filter when $K_L = 0$, and $\Delta L = 0$.

Figure 7a shows the output spectra of a notch filter with an equal 3 dB rejection bandwidth when $K_{12} = 0.2460$, $K_{11} = 0.4769$ and $K_{22} = 0.2528$, $K_{21} = 0.9483$. The two notch points are located at $\lambda_1 = 1550.2$ nm, and $\lambda_2 = 1550.3$ nm. The 3 dB rejection bandwidth of the two notch peaks are $\Delta\lambda_1 = \Delta\lambda_2 = 0.008$ nm.

Figure 8 shows the output spectra of the optical notch filter when K_{12}, K_{11}, K_{22} and K_{21} shift by a certain value independently. It can be seen that the parameters K_{12} and K_{11} determine the characteristics of the first notch point (1550.2 nm), while the parameters K_{22} and K_{21} determine the characteristics of the second notch point (1550.3 nm). The 3 dB bandwidth of the first and the second notch point can be tuned by the parameters K_{12} and K_{22} respectively. When K_{12} and K_{22} was decreased, the 3 dB bandwidth of the notch filter becomes narrower. The location of the first and the second notch point can be controlled by the parameters K_{11} and K_{21} respectively. When K_{11} and K_{21} was decreased, the location of
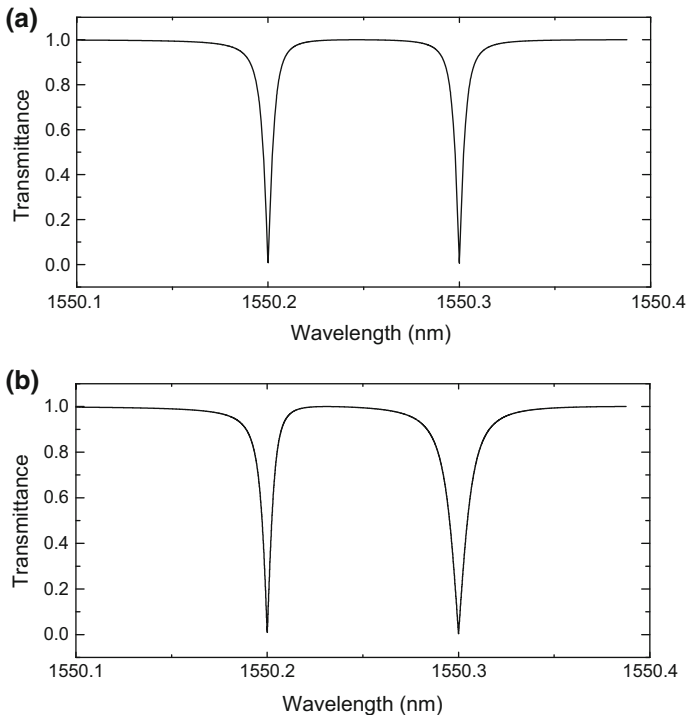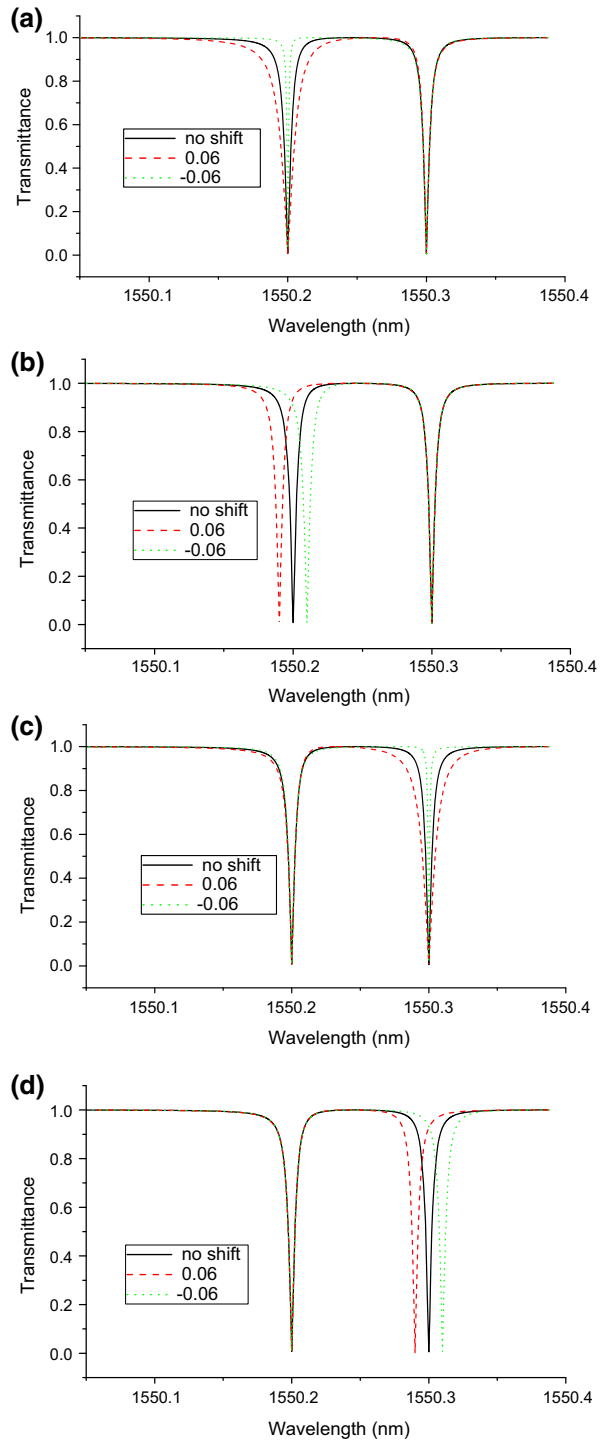

Fig. 7 The output spectra of a notch filter with **a** equal, and **b** unequal 3 dB rejection bandwidth

Fig. 8 The spectra response of a notch filter when parameters **a** K_{12}; **b** K_{11}; **c** K_{22}; **d** K_{21} shift independently
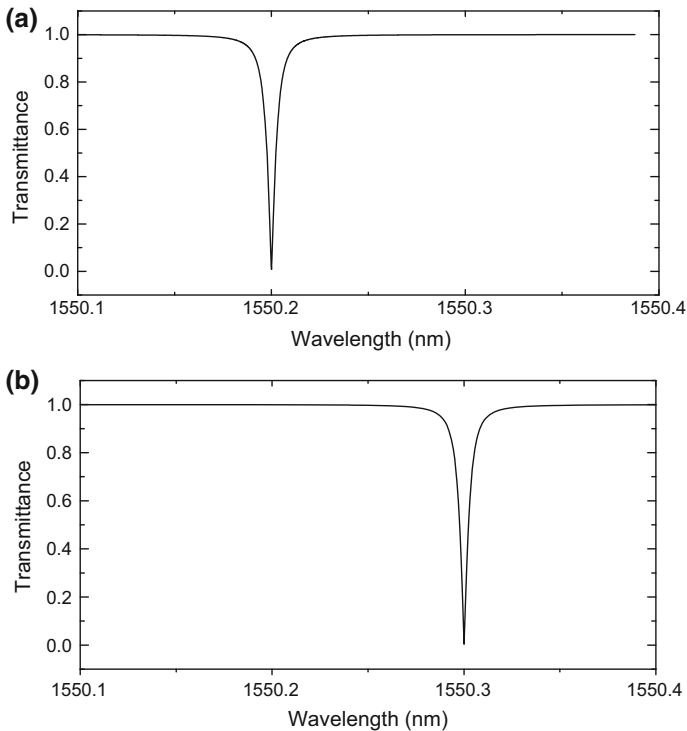
Fig. 9 The spectra response of the notch filters with notch points located at **a** 1550.2 nm; **b** 1550.3 nm

the notch points shifts to the long wavelength direction. The independent tunabilities of the bandwidth and notch locations make the structure more flexible in applications. Specific filtering properties can be obtained through adjusting corresponding parameters. For example, Figs. 7b and 8c shows the spectral response of a notch filter with unequal 3 dB rejection bandwidth ($\Delta\lambda_1 = 0.008$ nm, $\Delta\lambda_2 = 0.016$ nm) by adjusting K_{22}.

If only one double-ring resonator, such as the first double-ring resonator, is used in the structure (i.e. $K_{21} = K_{22} = 0$), a single notch point located at 1550.2 nm can be obtained, as shown in Fig. 9a. Similarly, when only the second double-ring resonator is used in the structure (i.e. $K_{11} = K_{12} = 0$), a single notch point located at 1550.3 nm can be obtained, as shown in Fig. 9b. More notch points can be obtained by coupling more double-ring resonators in the horizontal direction on the upper arm.

3.3 Poles/zeros figures for different filter responses

As we know, the poles of the transfer function amplify the frequency response while the zeros attenuate it. We can place poles and zeros on the unit circle and quickly evaluate the filter's frequency response. The poles/zeros plots of the multifunction filters are shown in Fig. 10. The corresponding frequency (spectral) response was also shown.
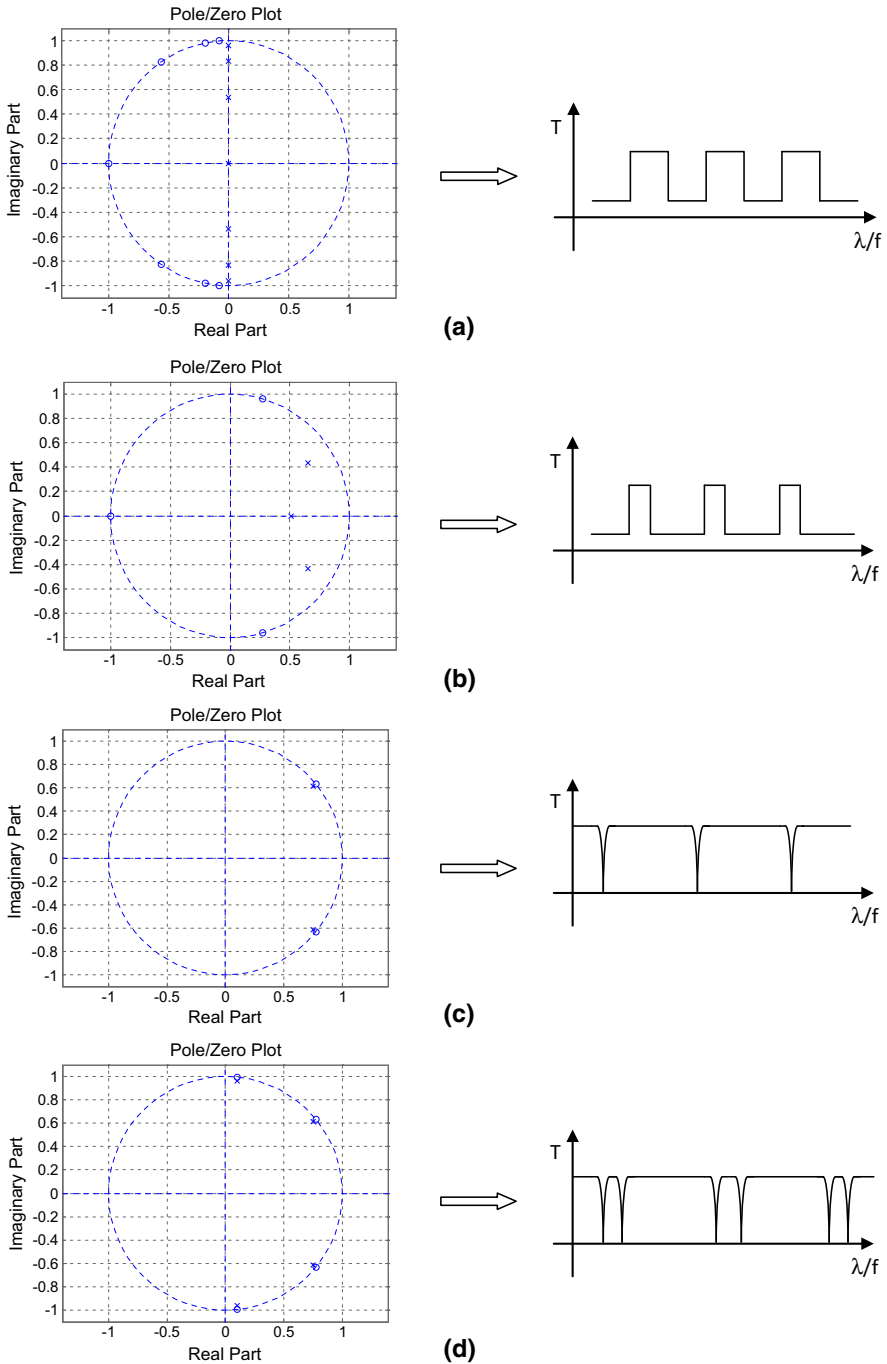
Fig. 10 The poles/zeros and frequency (spectral) responses of the multifunction filters. **a** symmetrical interleaver, **b** asymmetrical interleaver, **c** notch filter with a single notch point, **d** notch filter with two notch points

4 Fabrication analysis

The proposed multifunction filter can be fabricated based on planar light circuit (PLC) technology or micro-fiber technique. PLC technology is the most often used method for making micro-ring resonator. It is particularly suited for monolithic integration with other components. The detailed description of fabrication technique can be easily found in published literatures (such as Kohtoku et al. 2000).

The path length differences of the MZI, ring length of the resonators, and the coupling coefficients of the couplers are the key structural parameters of the proposed multifunction filter. Different parameters have different influences on the filtering characteristics. For example, there are five coupling coefficients, i.e. K_a, K_b, K_{11}, K_{12}, K_L, two length parameters, i.e. the length difference of the two arms of the MZI ΔL and the ring length of ring resonator l, in a symmetrical interleaver structure. The deviation of K_{11}, K_{12} and K_L from the ideal value will have more influence on the output spectra than that of K_a, K_b. Moreover, among K_{11}, K_{12} and K_L, the influence of K_{12} is the largest, K_L is less, and K_{11} is the least. For the length parameters, the condition $l/\Delta L = 2{:}1$ should be met in fabrication. Otherwise, the passband and stopband will not be flat any more. If ΔL and l changed synchronously keeping $l/\Delta L = 2{:}1$, the center frequency will shift although the output passband and stopband are still flat. The change of l is more sensitive than that of ΔL.

5 Conclusion

In this paper, a DSP method was used to synthesis a ring-resonator based multifunctional optical filter. The transfer function of the unbalanced Mach–Zehnder interferometric structure was deduced from its digital signal model obtained by the Z-transform method. This structure can function as a symmetrical interleaver, an asymmetrical interleaver with arbitrary duty cycles, a notch filter with a single notch point and a notch filter with two notch points, by simply tuning the structural parameters, such as the path length differences of the MZI, ring length of the resonators, and the coupling coefficients of the couplers. Computer-based DSP algorithms and technologies exhibit much advantage in the design of complex interferometric structures, such as multifunction filters used in the future intelligent DWDM networks.

References

Cheng, C.H.: Signal processing for optical communication. IEEE Signal Process. Mag. **23**(1), 88–96 (2006)
Cheng, C.H., Tang, S.: Michelson interferometer based interleaver design using classic IIR filter decomposition. Opt. Express **21**(25), 31330–31335 (2013)
Dingel, B.: Multifunctional optical filter using direct-coupled and cross-coupled all-pass filters. IEEE Photonics Technol. Lett. **26**(8), 785–788 (2014)
Dingel, B., Izutsu, M.: Multifunction optical filter with a Michelson–Gires–Tournois interferometer for wavelength-division-multiplexed network system applications. Opt. Lett. **23**(14), 1099–1101 (1998)

Kohtoku, M., Oku, S., Kadota, Y., Shibata, Y., Yoshikuni, Y.: 200-GHz FSR periodic multi/demultiplexer with flattened transmission and rejection band by using a Mach–Zehnder interferometer with a ring resonator. IEEE Photonics Technol. Lett. **12**(9), 1174–1176 (2000)

Little, B.E., Chu, S.T., Absil, P.P., Hryniewicz, J.V., Johnson, F.G., Seiferth, F., Gill, D., Van, V., King, O., Trakalo, M.: Very high-order microring resonator filters for WDM applications. IEEE Photonics Technol. Lett. **16**(10), 2263–2265 (2004)

Madsen, C.K.: General IIR optical filter design for WDM applications using all-pass filters. J. Lightwave Technol. **18**(6), 860–868 (2000)

Madsen, C.K., Zhao, J.H.: Optical Filter Design and Analysis: A Signal Processing Approach. John Wiley & Sons, New York (1999)

Mitra, S.K.: Digital Signal Processing: A Computer-Based Approach. McGraw-Hill, New York (2006)

Modarrerssi, A.R., Mohan, S.: Control and management in next-generation networks: challenges and opportunities. IEEE Commun. Mag. **38**(10), 94–102 (2000)

Pei, S.C., Tseng, C.C.: IIR multiple notch filter design based on allpass filter. IEEE Trans. Circuits Syst. **44**(8), 133–136 (1997)

Pinzon, P.J., Vazquez, C., Perez, I., Pena, J.M.S.: Synthesis of asymmetric flat-top birefringent interleaver based on digital filter design and genetic algorithm. IEEE Photonics J. **5**(3), 7100113 (2013)

Sun, Y., Fan, X.: Optical ring resonators for biochemical and chemical sensing. Anal. Bioanal. Chem. **399**(1), 205–211 (2011)

Xia, F., Rooks, M., Sekaric, L., Vlasov, Y.: Ultra-compact high order ring resonator filters using submicron silicon photonic wires for on-chip optical interconnects. Opt. Express **15**(19), 11934–11941 (2007)

Yang, X., Zhang, J.: Optimum design of asymmetric birefringent interleaver based on FIR digital filter design technique. In: Proceedings of 2008 China–Japan Joint Microwave Conference (CJMW2008), pp. 595–598 (2008)

Zhang, J.: Digital Signal Processing (DSP): Fundamentals, Techniques and Applications. Nova Science Publishers, New York (2016)

Zhang, J., Yang, X.: Universal Michelson Gires–Tournois interferometer optical interleaver based on digital signal processing. Opt. Express **18**(5), 5075–5088 (2010)

Zhang, J., Guo, S., Li, X.: General IIR optical notch filter based on Michelson Gires–Tournois interferometer. Opt. Commun. **285**(5), 491–496 (2012)

Zhang, J., Fu, W., Zhang, R., Wang, Y.: Description and reconstruction of one-dimensional photonic crystals by a digital signal processing theory. Chin. Phys. B **23**(10), 104215 (2014)